Water vapor in hydrogen flames measured by time-resolved collisional dephasing of the pure-rotational N_2 CARS signal

Castellanos, Leonardo; Mazza, Francesco; Bohlin, Alexis

DOI
10.1016/j.proci.2022.09.001

Publication date
2022

Document Version
Final published version

Published in
Proceedings of the Combustion Institute

Available online at www.sciencedirect.com

ScienceDirect

Proceedings of the Combustion Institute 39 (2023) 1279–1287

Proceedings of the Combustion Institute

www.elsevier.com/locate/proci

Water vapor in hydrogen flames measured by time-resolved collisional dephasing of the pure-rotational N_2 CARS signal

Leonardo Castellanos [a], Francesco Mazza [a], Alexis Bohlin [a,b,*]

[a] *Ultrafast Laser Diagnostics and Flames Laboratory, Faculty of Aerospace Engineering, Delft University of Technology, Kluyverweg 1, Delft 2629 HS, the Netherlands*

[b] *Space Propulsion Laboratory, Department of Computer Science, Electrical and Space Engineering, Luleå University of Technology, Bengt Hultqvists väg 1, Kiruna 98128, Sweden*

Received 20 December 2021; accepted 1 September 2022
Available online 20 October 2022

Abstract

We present a novel diagnostic technique to probe water vapor (H_2O) concentration in hydrogen (H_2) combustion environments via the time-resolved measurement of the collisional dephasing of the pure-rotational coherent anti-Stokes Raman scattering (CARS) signal of nitrogen (N_2). The rotational Raman coherence of the N_2 molecules, induced by the interaction with the pump and Stokes laser fields, dephases on a timescale of hundreds of picoseconds (ps), mostly due to inelastic collisions with other molecules in atmospheric flames. In the spatial region of H_2 flames where H_2O is present in appreciable amount, it introduces a faster dephasing of the N_2 coherence than the other major combustion species do: we use time-resolved femtosecond/picosecond (fs/ps) CARS to deduce the H_2O mole fraction from the dephasing effect of its inelastic collisions with N_2. The proof-of-principle is demonstrated in a laminar H_2/air diffusion flame, performing sequential measurements of the collisional dephasing of the N_2 CARS signal up to 360 ps. We measure the temperature and the relative O_2/N_2 and H_2/N_2 concentrations at a short probe delay, and input the results in the time-domain model to extract the H_2O mole fraction from the signal decay, thus measuring the whole scalar flow fields across the flame front. We furthermore present single-shot simultaneous thermometry and absolute concentration measurements in the turbulent TU Darmstadt/DLR Stuttgart canonical 'H3 flame' performed by dual-probe CARS measurements obtained with a polarization separation approach. This allows us to probe the molecular coherence simultaneously at ∼20 and ∼250 ps on the basis of a single-laser-shot, and record the resulting signals in two distinct detection channels of our unique polarization-sensitive coherent imaging spectrometer. The proposed technique allows for measuring the absolute concentrations of all the major species of H_2 flames, thus providing a full characterization of the flow composition, as well as of the temperature field.

* Corresponding author at: Space Propulsion Laboratory, Department of Computer Science, Electrical and Space Engineering, Luleå University of Technology, Bengt Hultqvists väg 1, Kiruna 98128, Sweden.
E-mail address: alexis.bohlin@ltu.se (A. Bohlin).

https://doi.org/10.1016/j.proci.2022.09.001

Keywords: Time-resolved spectroscopy; fs/ps CARS thermometry; Water vapor detection; Absolute species concentration measurements; Hydrogen combustion

1. Introduction

Coherent anti-Stokes Raman spectroscopy (CARS) is a laser diagnostic technique that has found vast application to the experimental investigation of combustion processes, owing to the possibility of performing *in-situ*, non-perturbative measurements, with excellent spatial and temporal resolution [1]. CARS is currently the gold-standard for high-fidelity thermometry in gas-phase reacting flows [2], and is employed in many measurement scenarios of practical interest, such as internal combustion engines [3,4] gas-turbine engines [5,6], rocket combustors [7] and detonation processes [8]. In addition to thermometry, CARS has been extensively applied to the detection of major combustion species [9,10], performing relative concentration measurements on both ro-vibrational [11] and pure rotational [12] Raman spectra, and even absolute concentration measurements have been demonstrated [13].

A recognized challenge for absolute concentration measurements in combustion environments is to detect water vapor (H_2O): this is typically achieved through absorption spectroscopy [14] rather than Raman-based techniques, owing to its relatively low Raman cross section [15]. An inherent drawback of absorption spectroscopy is the limitation to line-of-sight measurements: the development of non-linear optical diagnostics could thus provide *in-situ* H_2O measurements with spatial resolution. In the context of hydrogen combustion, H_2O plays a key role as it is the only major product: quantitative measurements of the H_2O concentration and local temperature thus allow for mapping the progress of the chemical reaction. In this respect, the H_2O mass fraction typically plays a key role in the definition of the progress variable employed in numerical codes, e.g. based on flamelet-generated manifolds [43]. O'Byrne et al. [16] employed CARS to measure the temperature and the mole fractions of nitrogen (N_2), oxygen (O_2), and hydrogen (H_2) in a supersonic combustor, and estimated the H_2O concentration by assuming it to be the only other major species contributing to the non-resonant susceptibility of the gas-phase medium. Direct measurements of the ro-vibrational CARS spectrum of the H_2O v_1 symmetric stretch at $\sim$3650 cm^{-1} have been first attempted by Hall et al. [17] in 1979. Hall and Sherley [18], as well as Porter and Williams [19], performed ro-vibrational H_2O CARS thermometry at temperatures as high as 2000 K. Greenhalgh et al. also investigated the H_2O v_1 CARS spectrum at high temperatures and elevated pressures [20]. Despite the good agreement shown by the experimental data and the theoretical CARS models, further studies on this spectrum were scarce, probably owing to the isolated location of the H_2O v_1 spectrum beyond the vibrational fingerprint region, which hinders the simultaneous detection of multiple species. In this sense, the application of CARS spectroscopy to the pure-rotational spectrum of gas-phase H_2O is more appealing for combustion diagnostics. This was attempted for the first and only time by Nordström et al. [21]: unfortunately, they concluded that H_2O is an unsuitable candidate for CARS concentration measurements in combustion, due to the signal intensity being more than five orders of magnitude smaller than that of N_2. The extreme dimness of the pure-rotational H_2O CARS signal was attributed to both its low Raman cross section and to the large number of rotational transitions of this asymmetric top molecule, characterized by three distinct principal moments of inertia [22].

In the present work, we demonstrate the use of time-resolved CARS to measure the H_2O mole fraction in laboratory flames, through its impact on the pure-rotational N_2 spectrum. Nordström et al. pointed out in the conclusion of their work that, despite its CARS spectrum being negligible, water vapor has a significant collisional impact on the N_2 CARS spectrum, as demonstrated experimentally in [21]. Rotational energy transfer (RET) in inelastic collisions between the coherently excited N_2 molecules and other molecules results in the temporal dephasing of the pure-rotational N_2 CARS signal on a time-scale of picoseconds (ps) at ambient conditions. The development, in recent years, of CARS techniques employing ultrashort laser pulses to resolve the temporal evolution of the Raman coherence [23] opened to the possibility of measuring the collisional RET in the time domain [24]. Here we employ hybrid femtoseconds/picosecond (fs/ps) CARS [25] to measure the dephasing of the pure-rotational N_2 CARS signal due to inelastic collisions with the H_2O molecules in H_2/air flames. The proof-of-principle measurements are performed across a laminar H_2/air diffusion flame, provided on a Bunsen burner. The applicability of the proposed technique to single-shot measurements in turbulent flames is further demonstrated by using single-shot

dual-probe CARS [26] in the canonical H3 flame [27].

2. Theoretical considerations

Hybrid fs/ps CARS employs ultrashort laser pulses to perform simultaneously time- and frequency-resolved ro-vibrational spectroscopy on the Raman-active molecules. Broadband fs pulses provide the pump and Stokes photons, whose frequency difference coherently excite the molecules to higher rotational energy states according to the selection rule: $\Delta v = 0$ and $\Delta J = +2$ (for the pure-rotational S-branch spectrum), where v is the vibrational quantum number, and J is the total angular momentum quantum number. The use of fs pulses further allows for a great simplification of the experimental setup, as a single combined pump/Stokes pulse can be employed to simultaneously deliver the constructive pump/Stokes photon-pairs, which are found across its broad bandwidth [28]. In addition, by using fs pulses with duration lesser than about one tenth of the molecular rotational period (i.e. ~500 fs for N_2), we can maximize the rotational Raman coherence in the medium, through its impulsive excitation [29]. In our setup, we employ a ~35 fs transform-limited (TL) pump/Stokes pulse to excite the rotational Raman coherence of the N_2 molecules, described on a macroscopic scale by the third-order non-linear optical susceptibility of the medium (χ_{CARS}). A relatively narrowband ~12 ps probe pulse is then coherently scattered by the medium resulting in the generation of the CARS signal. The probe pulse is delayed with respect to the pump/Stokes pulse both to time-gate the generation of the non-resonant background and, for the purpose of this work, to measure the collisional dephasing of the Raman signal. The time-domain third-order susceptibility is then the interferogram resulting from the harmonics corresponding to the different Raman frequencies, as:

$$\chi_{CARS} = \sum_{v}\sum_{J} W_{v,J\to v,J+2} \cdot \exp\left[\left(i\omega_{v,J\to v,J+2} - \Gamma_{v,J\to v,J+2}\right)t/(2\pi c)\right] \quad (1)$$

where $W_{v,J\to v,J+2}$, $\omega_{v,J\to v,J+2}$, and $\Gamma_{v,J\to v,J+2}$ are respectively the overall probability, the Raman frequency and the temporal dephasing coefficient associated to each pure-rotational S-branch transition (i.e. $J \to J+2$). The temporal evolution of χ_{CARS} is thus determined by the interference of the Raman modes corresponding to transitions from different J states, as well as by the dephasing coefficients associated to the transitions. These account for the spontaneous emission from the coherent molecules and for the effect of decoherence due to molecular collisions. The natural decay lifetime of N_2 is on the order of seconds due to symmetry constrains [30], so that it can be neglected in our discussion. As for the collisional dephasing, the effect of pure dephasing due to elastic collisions ($\Delta J = 0$) can be neglected at ambient pressure [30], so that the main contribution stems from inelastic collisions ($\Delta J \neq 0$), responsible for the RET between the coherently excited N_2 molecules and the molecular colliders in the flame. The collisional RET is both state-dependent and species-specific, owing to the spacing of the J states in the ro-vibrational energy manifold of the colliding molecules. In the present work, we account for the dephasing of the N_2 CARS signal due to collisions with the following perturbers in H_2/air flames: N_2-N_2 (i.e. self-perturbed) [31], N_2-O_2 [32], N_2-H_2 [33], and N_2-H_2O [34]. Figure 1 shows the corresponding state-dependent dephasing coefficients for J = 0-60: while the N_2-N_2 and N_2-O_2 coefficients show a comparable J-dependence, owing to the similar rotational energy manifold, both N_2-H_2 and N_2-H_2O coefficients show peculiar trends over the different J states and have an overall larger magnitude. The J-dependence of the N_2-H_2 coefficients is less pronounced than for the other collisional partners, due to the large spacing between the states in the rotational energy manifold of H_2, resulting in a similarly reduced RET for all the J states of the N_2 molecule. On the other hand, the overall large magnitude of these coefficients is explained by the larger thermal velocity of the lightweight H_2 molecule, allowing it to penetrate closer to the repulsive wall of the interaction potential with the N_2 molecule [33]. The N_2-H_2O dephasing coefficients are characterized by a strongly non-monotonic J-dependence, with a temperature-dependent local maximum (e.g. $J = 24$ at 1600 K), which is attributed to the complex structure of the rotational energy manifold of the H_2O molecule, resulting in a strong dependence of the RET on the initial rotational state of the N_2 molecule [34].

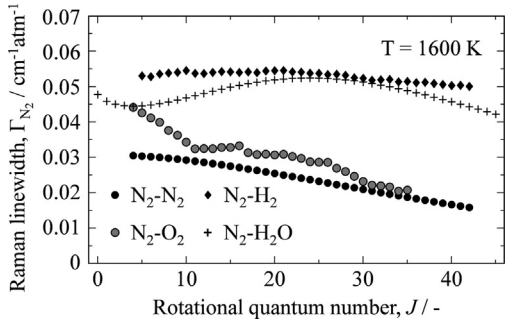

Fig. 1. The J-dependence of the species-specific N_2 CARS dephasing coefficients, for inelastic collisions with the major combustion species in H_2/air flames (i.e. N_2, O_2, H_2, and H_2O) at $T = 1600$ K.

The total N_2 dephasing coefficients are then computed as:

$$\Gamma^{N_2}_{J\rightarrow J+2} = \sum_k X_k \cdot \Gamma_{J\rightarrow J+2}(N_2 - M_k) \quad (2)$$

where $\Gamma_{J\rightarrow J+2}$ are the dephasing coefficients due to collisions of N_2 with the kth perturber, weighted by its mole fraction. Eq. (2) then introduces the dependence of the N_2 CARS signal on the H_2O mole fraction, which is employed in the present work to measure the H_2O concentration in H_2/air flames. In this context, the collisional environment can be interpreted as an equivalent binary system composed of H_2O on one hand, and a weighted combination of all other perturber species whose concentration is directly measured in the frequency domain (i.e. N_2, O_2 and H_2) on the other:

$$\Gamma^{N_2}_{J\rightarrow J+2} = \sum_{k'} X_{k'} \cdot \Gamma_{J\rightarrow J+2}(N_2 - M_{k'}) + X_{H_2O} \cdot \Gamma_{J\rightarrow J+2}(N_2 - H_2O) \quad (3)$$

The proposed diagnostic approach can thus be employed to measure the H_2O concentration in all combustion environments where the concentration of every other relevant collisional partner is accessible in the CARS spectrum.

3. Experimental methodology

3.1. Laminar flame experiment

The proof-of-principle demonstration of H_2O concentration measurements through the dephasing of the N_2 CARS signal is performed in a laminar H_2/air diffusion flame. The two-beam fs/ps CARS system is described in details in [35]: only a brief summary is presented here. A single regenerative laser amplifier system (Astrella, Coherent) provides ~35 fs (full-width-at-half-maximum, FWHM) pulses at 800 nm, with a total pulse energy of ~7.5 mJ, at 1 kHz repetition rate. The narrowband ps probe pulse is generated at ~403 nm by a second-harmonic bandwidth compressor (SHBC, Light Conversion) fed by a 65% portion slip off the fs laser output. A 4f-filter in transmission is placed in the probe beam path to tune the duration of the pulse: in the present work we set a probe duration of ~12 ps FWHM, with ~300 μJ/pulse, which corresponds to a FWHM bandwidth of ~2.7 cm^{-1}. The resulting spectral resolution is nearly two orders of magnitude larger than the N_2-H_2O Raman linewidths at the flame temperature, as shown in Fig. 1, and it prevents the direct measurement of the H_2O concentration in the frequency domain, by its broadening effect on N_2 lines in the CARS spectrum. The combined fs pump/Stokes pulse originates from the remainder 35% portion of the amplifier output, corresponding to 2.5 mJ/pulse; an external compressor unit is employed to compensate for the optical dispersion terms arising along the beam path, ensuring a TL pulse at the measurement location. The pump/Stokes and probe pulses are therefore automatically synchronized, and an automated delay stage (sub-10 fs resolution, Thorlabs) is employed to control the relative probe pulse delay. Spherical optics (f : = 500 mm and 300 mm, respectively) focus the pump/Stokes and probe beams to the measurement location, and the crossing angle for the two-beam phase matching configuration is estimated to be ~3°, resulting in the following probe volume dimensions: ~22 μm (height) x ~1.1 mm (length) x ~22 μm (width). Half-wave plates for 400 and 800 mm are used to control the relative polarization of the two laser pulses and, in combination with a thin-film polarizer, to attenuate the pump/Stokes energy to ~60 μJ/pulse and avoid fs laser-induced filamentation [36]. This was verified by performing a power scaling of N_2 CARS signal at room temperature: at this fluence level no change in the spectral envelope was observed. A wedge prism is inserted in the pump/Stokes beam path after the probe volume, and the low-power reflection is imaged onto a beam profiler (WinCamD, Dataray) in the far-field to monitor and maintain the alignment of the pump/Stokes beam when moving the delay stage. The CARS signal is collected in a coherent imaging spectrometer constituted by a relay-imaging telescope (f : = 400 mm) combined with a high-dispersion transmission grating (3039 l/mm, Ibsen Photonics), allowing the detection of the CARS signal over the range ~50–600 cm^{-1}, with 0.25 cm^{-1}/pixel, by the sCMOS detector (Zyla, Andor). The pure-rotational CARS spectra of N_2 and O_2 are thus recorded along with the first two rotational lines of the pure-rotational H_2 CARS spectrum, enabling the measurement of the relative O_2/N_2 and H_2/N_2 concentrations.

The proof-of-principle demonstration of H_2O concentration measurements via time-domain N_2 CARS is performed in a laminar N_2-diluted H_2/air diffusion flame, provided on a Bunsen burner. The burner is made of a seamless, stainless steel pipe with ~19 mm inner diameter; a N_2-H_2 mixture (50%–50% in volume) is inlet with a bulk velocity of ~1 m/s, resulting in a Reynolds number < 150. A stainless steel mesh is placed over the burner at a height-above-the-burner (HAB) of ~30 mm, to stabilize the flame. The CARS measurements were performed at ~1 mm HAB, performing a radial scan from the center of the burner ($y = 0$ mm) and past the rim, with data-points acquired every 0.5 mm up to $y = 12$ mm. At each measurement location 6 datasets of 1000 single-shot CARS spectra were acquired for a probe delaying varying from 30 to 360 ps. The spectra acquired at the lowest probe delay were employed to measure the temperature and the relative O_2/N_2 and H_2/N_2 concentrations. Neglecting the effect of collisions at the short probe delay timescale leads to an inaccuracy of less than

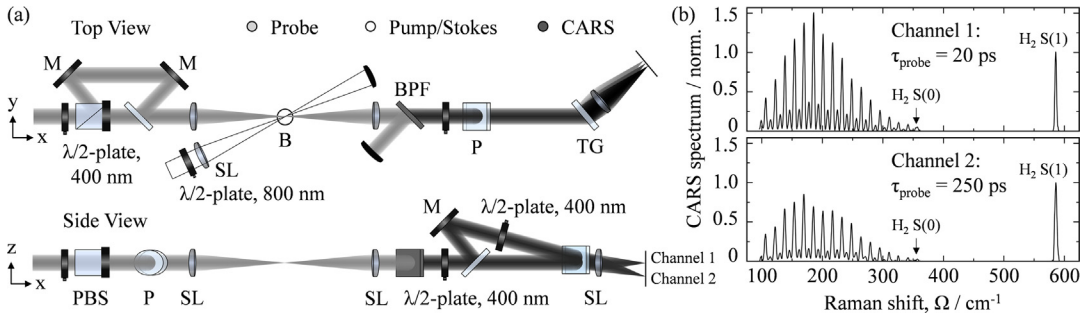

Fig. 2. (a) Schematic of the experimental setup employed for single-shot dual-probe CARS measurements in the H3 flame. A polarization beam splitter (PBS) and a thin-film polarizer (P) are employed to split the probe in two pulses with orthogonal polarization and an recombine them with an intra-pulse delay of 230 ps. The cross-polarized CARS signals are simultaneously collected in two distinct detection channels in the polarization-sensitive coherent imaging spectrometer. λ/2-plate, half-wave plates; M, mirrors; SL, spherical lenses; BPF, band-pass filter; TG, transmission grating; B, burner. (b) Single-shot CARS spectra simultaneously generated at 20 and 250 ps in the fuel stream of the laminar H_2/air diffusion flame, and recorded in the two detection channels. Both spectra are normalized with respect to the S(1) rotational line of H_2, at 587 cm^{-1}.

~0.8% in the estimated temperature: the CARS signal generated at this delay is thus assumed as nearly collisional independent. By integrating the N_2 CARS signal acquired at the longer probe delays the collisional dephasing was measured and compared to the single-exponential decay model in Eqs. (1) and (2) to extract the H_2O mole fraction (see Fig. 3).

3.2. Turbulent flame experiment

The methodology described in the previous section requires sequential measurements of the N_2 CARS signal at increasing probe delays and is thus not suitable to measurements in turbulent flames, where the temperature and chemical composition of the flow are highly dynamic. This limitation can be overcome by employing dual-probe CARS, i.e. by splitting the probe pulse and controlling the delay relative to the pump/Stokes pulse, so as to simultaneously perform a collisional-independent measurement at short probe delay and a time-resolved measurement of the RET at longer probe delays. This approach was first demonstrated by Patterson et al. to perform single-shot measurements of the collisional dephasing of the S-branch N_2 CARS spectrum [26], and subsequently employed to perform CARS pressure measurements in 0-D and 1-D configurations [37–40]. In the present work we demonstrate for the first time the use of a polarization separation approach to achieve dual-probe CARS measurements. The experimental setup described in the previous section is slightly modified as depicted in Fig. 2(a). A Glan-Taylor polarization beam splitter (PBS) is mounted on the probe beam path after the 4f-filter with horizontal transmission axis and a 400 nm half-wave plate tunes the ratio of the polarization splitting. The vertically-polarized component of the probe beam is reflected by the PBS and directed to a retroreflector mounted on a linear translation stage to control the relative delay of the two probe pulses: in the present work an intra-pulse delay of ~230 ps was employed. A thin-film polarizer mounted at Brewster's angle is then used to recombine the two cross-polarized probe pulses on the same beam path. The polarization-sensitive coherent imaging spectrometer described in [41] is employed to simultaneously detect the cross-polarized signals in two distinct detection channels. Figure 2(b) present an example of the two single-shot spectra simultaneously generated at 20 and 250 ps in the fuel stream of the laminar H_2/air diffusion flame. The effect of molecular collisions after 250 ps is visible on the envelope of the pure-rotational N_2 CARS spectrum, as well as on the differential dephasing of the pure-rotational H_2 signal characterized by a much lesser RET rate. The balanced detection of the dual-probe CARS setup is performed by changing the pump/Stokes beam path-length to generate the signal (in a room-temperature N_2 flow) with the two probe pulses at the same relative delay, accounting both for the polarization-dependent signal generation efficiency and for the transmission efficiency of the two detection channels. This approach guarantees the automatic overlap of the two probe pulses at the measurement location and minimizes the uncertainty due to phase-mismatch of the degenerate pump/Stokes and probe beams, which can significantly impact the intensity of the second H_2 line at higher Raman shifts.

We demonstrate single-shot H_2O concentration measurements in the TU Darmstadt/DLR Stuttgart H3 flame, which is a canonical turbulent non-premixed H_2/air flame [27]. The burner consists of a straight stainless-steel tube, with 8 mm inner diameter (D) and a tapered rim at the exit, and a concentric contoured nozzle, with an inner

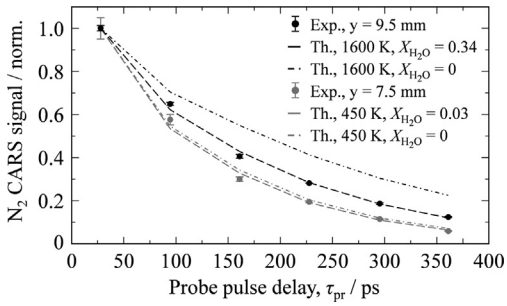

Fig. 3. Experimental measurement of the N_2 CARS signal collisional dephasing at two locations in the reaction zone of the laminar H_2/air flame. The experimental decay is compared to the time-domain CARS model to extract the H_2O mole fraction, resulting in $X_{H2O} = 0.03$ at $y = 7.5$ mm (grey), and $X_{H2O} = 0.34$ at $y = 9.5$ mm (black).

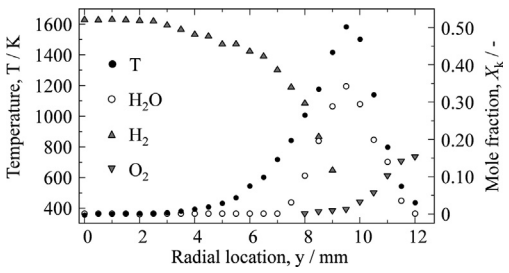

Fig. 4. Experimental profiles of the temperature and mole fractions of the major combustion species across the flame front of the laminar H_2/air diffusion flame. The measured H_2O mole fraction at 1 mm HAB varies in the range $X_{H2O} = 0.03$–0.34 in the reaction zone y = 7.5–11.5 mm.

diameter of 140 mm, providing a coflow of dry air. Digital flow controllers (Bronkhorst) are employed to regulate the volumetric flows of N_2 and H_2, constituting a 50%–50% (in volume) mixture provided through the center pipe of the burner with an exit speed of 34.8 m/s, resulting in a turbulent flow with Re = 10000, as well as the air coflow. The burner is mounted on translation stages to control its axial and radial position, and measurements are performed at a HAB of 20 mm ($z/D = 2.5$).

4. Results and discussion

4.1. Laminar flame measurements

At each radial location across the laminar H_2/air flame front we performed N_2 CARS thermometry and relative O_2/N_2 and H_2/N_2 concentration measurements on the spectra acquired at the shortest probe delay (i.e. 30 ps). At such early temporal delay the effect of inelastic collisions can be taken to be negligible, at atmospheric pressure. Once the temperature and the relative O_2/N_2 and H_2/N_2 concentrations are known, their experimental values are employed to generate a library of synthetic CARS spectra for varying relative H_2O/N_2 concentrations. The experimental N_2 CARS spectra are integrated in the spectral range ~120–230 cm^{-1}, corresponding to the N_2 lines $J = 14$–28, to avoid interference with the O_2 lines, and compared to the theoretical dephasing to measure the H_2O mole fraction. Figure 3 shows the experimental dephasing measured at two locations in the reaction zone and compared to the theoretical dephasing curves predicted by the time-domain N_2 CARS code for $X_{H2O} = 0$ and for the best-fit value. The black curves represent the signal dephasing at y = 9.5 mm (at 1 mm above the burner rim), where the H_2O mole fraction is measured to be 0.34 according to the best-fitting curve: a large sensitivity to the H_2O concentration is shown by the significant bias between the experimental data and the theoretical dephasing predicted for $X_{H2O} = 0$. At y = 7.5 mm (grey curves) the H_2O mole fraction is reduced to 0.03, which represents the H_2O detection limit in the present work as a minimal deviation between the best-fit and the $X_{H2O} = 0$ theoretical curves is observed.

The methodology just explained is employed to measure the whole temperature and chemical composition fields across the flame front. Figure 4 shows the resulting experimental profiles for the temperature and the mole fractions of O_2, H_2 and H_2O. The temperature smoothly increases from ~360 K in the fuel stream at the center of the burner ($y = 0$ mm), peaking to 1620 K above the burner rim ($y = 9.5$ mm), and decreases more rapidly in the lean reaction zone reaching ~440 K in the oxidizer stream at $y = 12$ mm. The good single-shot precision of the CARS thermometry, varying in the range 0.8–3.7% in the high-temperature reaction zone, indicates a limited impact of the temperature fluctuations on the signal intensity, thus justifying the use of sequential measurements of the collisional dephasing for the laminar flame case. The H_2 mole fraction decreases from ~52% in the fuel stream at the center of the burner as the mixing and chemical reaction progress toward the burner rim. The simultaneous detection of the pure-rotational N_2 CARS spectrum and of two rotational lines of the pure-rotational H_2 CARS spectrum, namely S(0) at 354 cm^{-1} and S(1) at 587 cm^{-1}, allows for measuring the relative H_2/N_2 concentration at temperatures as high as 1450 K at location $y = 9$ mm. The O_2 mole fraction, on the other hand, smoothly grows from 0.01 measured at y = 8 mm up to 0.15 at the last measurement location in the oxidizer stream. The relative standard deviation of the measured mole fractions of H_2 and O_2 is, respectively, lesser than 2.5 and 8% at all measurement locations. H_2O is detected in the reaction zone, for $y = 7.5$–11.5 mm, with a maximum mole fraction of 0.34 at

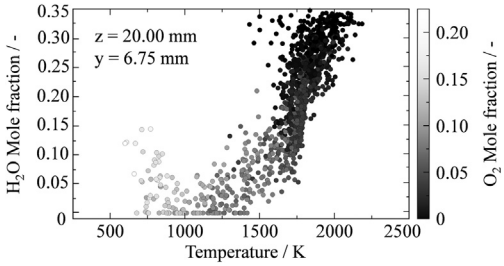

Fig. 5. Scatter plot of the H_2O mole fraction *versus* temperature measured by the 1200 single-shot CARS spectra acquired at the location with the highest temperature in the turbulent H3 flame. The grayscale color represents the measured O_2 mole fraction.

y = 9.5 mm. The uncertainty in the measured H_2O concentrations is mostly due to shot-to-shot fluctuation in the temperature and flow composition. This was assessed by propagating the uncertainty in the measured temperature and relative O_2/N_2 and H_2/N_2 concentrations and fitting the experimental data to the corresponding limit curves for the theoretical dephasing. The relative uncertainty in the H_2O mole fraction is thus estimated to be <8% at all measurement locations, with the sole exception of $y = 10.5$ mm, where the relative uncertainty is 15%, corresponding to a measured H_2O mole fraction in the range 0.18–0.21.

The temperature and mole fraction profiles in Fig. 4 are in good qualitative and quantitative agreement with those reported by Toro et al. for a similar laminar H_2/air diffusion flame [42], and moreover show the effect of preferential diffusion of H_2 in the fuel stream. In the region $y = 2.5$–6.5 mm, the H_2 mole fraction reduces from 0.52 to 0.42, while no water vapor is detected, and the temperature is only slightly increasing due to heat transfer from the reaction zone, yet remaining below the auto-ignition threshold. The simultaneous resolution of the local temperature and composition fields thus allows us to render the physics of mass transport in the laminar diffusion flame.

4.2. Turbulent flame measurements

Single-shot detection of water vapor concentration is demonstrated in the turbulent H3 flame, as described in Section 3.2. Four samples of 300 single-shot CARS spectra were acquired at a radial location 6.75 mm from the centerline of the flame, at the highest temperature in the oxidizer stream.

The scatter plot in Fig. 5 shows the measured H_2O mole fraction *versus* temperature at the chosen flame location, while the grayscale color of each data-point represents the local O_2 mole fraction. The latter shows an inverse correlation to the local temperature, with the O_2 mole fraction increasing at lower temperatures. Similarly, the measured H_2O mole fraction has a clear correlation to the temperature in the reaction zone of the turbulent flame, with the concentration increasing with the local progress of the reaction in the probe volume. The clustering of the data-points showing high H_2O mole fraction at high temperatures is in good agreement with the original measurements performed by Meier et al. on the H3 flame [27]. At lower temperature, when a significant concentration of O_2 is present in the probe volume, the measured H_2O mole fraction shows a more spurious correlation, which is probably due to the beating of the N_2 lines employed in the measurement with O_2 lines. One additional caveat in the single-shot CARS measurements of the H_2O concentration is that the collisional dephasing of the N_2 CARS signal could only be measured at two probe delays. Further research effort should be spent on the investigation of the *J*-dependence of the collisional dephasing coefficients as an additional source of sensitivity to H_2O mole fractions, also to enhance the robustness of the measurements.

5. Conclusions

We have successfully demonstrated a novel time-resolved CARS diagnostic technique to quantify water vapor concentrations in hydrogen combustion environments. The technique relies on the use of relatively short ps probe pulses, following impulsive excitation, to realize measurements of the evolution and decay of the Raman coherence over a timescale of hundreds of ps. The dephasing of the pure-rotational N_2 CARS signal due to inelastic collisions with the H_2O molecules introduces a strong sensitivity to water vapor concentration. Coherent Raman-based detection of H_2O is otherwise very challenging, given the overall low Raman cross section of H_2O.

Proof-of-principle measurements of the H_2O concentrations were performed across the flame front of a laminar H_2/air diffusion flame. We recorded the pure-rotational N_2 CARS signals at six different probe delays relative to the pump/Stokes pulse, from 30 to 360 ps, and analyzed the corresponding collisional dephasing of the signal. The fs/ps CARS spectrum spans up to ~600 cm^{-1} allowing the simultaneous measurement of the temperature and of the relative O_2/N_2 and H_2/N_2 concentrations. The successful measurement of the H_2O concentration thus allowed to map the chemical composition of the flow across the H_2/air flame front, by measuring the absolute concentrations of the major combustion species.

Single-shot measurements in the turbulent H3 flame are presented by dual-probe fs/ps CARS, obtained with polarization control over the signal generation. The probe pulse is split in two pulses with an intra-pulse delay of ~230 ps and linear polarization set to be parallel and orthogonal to

the polarization of the pump/Stokes pulse. The N_2 CARS signal is thus simultaneously generated at ~20 and ~250 ps on the principle of a single-laser-shot; the cross-polarized signals are recorded in two distinct detection channels with our polarization-sensitive coherent imaging spectrometer. A total of 1200 single-shot CARS spectra were recorded at the highest temperature location in the oxidizer stream, at a HAB of 20 mm. The simultaneous measurement of the H_2O, O_2, H_2, and N_2 mole fractions, as well as temperature, was realized at this flame location. The statistical correlation of the measured quantities is in good agreement with experimental data available for this canonical flame, thus proving the applicability of the proposed technique to turbulent flames.

The novel CARS approach presented here has promising applications as an all-round laser diagnostic technique for scalar measurements in hydrogen flames, allowing for the simultaneous mapping of the temperature and chemical composition of the flow. Furthermore, its extension to more complex combustion environments, where a larger number of collisional partner is present, some of which might not be directly detected in the CARS spectrum, is an active research topic in our group.

Declaration of Competing Interest

The authors declare that they have no known competing financial interests or personal relationships that could have appeared to influence the work reported in this paper.

Acknowledgments

We gratefully acknowledge the financial support provided by the Netherlands Organization for Scientific Research (NWO), obtained through a Vidi grant in the Applied and Engineering Sciences domain (AES) (15690). In addition, A. Bohlin is thankful for support through the RIT (Space for Innovation and Growth) project/European Regional Development Fond in Norrbotten, Sweden.

References

[1] A.C. Eckbreth, Laser Diagnostics for Combustion Temperature and Species, 2nd ed., Gordon and Breach Publishers, 1996.
[2] S. Roy, J.R. Gord, A.K. Patnaik, Recent advances in coherent anti-Stokes Raman scattering spectroscopy: fundamental developments and applications in reacting flows, Prog. Energy Combust. Sci. 36 (2010) 280–306.
[3] C. Brackmann, J. Bood, M. Afzelius, P.-E. Bengtsson, Thermometry in internal combustion engines via dual-broadband rotational coherent anti-Stokes Raman spectroscopy, Meas. Sci. Technol. 15 (2004) 13–15.
[4] D. Escofet-Martin, A.O. Ojo, N.T. Mecker, M.A. Linne, B. Peterson, Simultaneous 1D hybrid fs/ps rotational CARS, phosphor thermometry, and CH* imaging to study transient near-wall heat transfer processes, Proc. Combust. Inst. 38 (2021) 1579–1587.
[5] T.R. Meyer, S. Roy, R.P. Lucht, J.R. Gord, Dual-pump dual-broadband CARS for exhaust-gas temperature and CO_2–O_2–N_2 mole-fraction measurements in model gas-turbine combustors, Combust. Flame 142 (2005) 52–61.
[6] M. Scherman, R. Santagata, E. Lin, P. Nicolas, J.P. Faleni, A. Vincent-Randonnier, P. Cherubini, F. Guichard, A. Mohamed, D. Gaffie, B. Attal-Tretout, A. Bresson, 1-kHz hybrid femtosecond/picosecond coherent anti-Stokes Raman scattering thermometry of turbulent combustion in a representative aeronautical test rig, J. Raman Spectrosc. 52 (2021) 1643–1650.
[7] F. Grisch, P. Bouchardy, W. Clauss, CARS thermometry in high pressure rocket combustors, Aerosp. Sci. Technol 7 (2003) 317–330.
[8] D.R. Richardson, S.P. Kearney, D.R. Guildenbecher, Post-detonation fireball thermometry via femtosecond-picosecond coherent anti-Stokes Raman Scattering (CARS), Proc. Combust. Inst. 38 (2021) 1657–1664.
[9] H. Zhao, Z. Tian, Y. Li, H. Wei, Hybrid fs/ps vibrational coherent anti-Stokes Raman scattering for simultaneous gas-phase, Opt. Lett. 46 (7) (2021) 1688–1691.
[10] Y. Ran, A. Boden, F. Küster, F. An, A. Richter, S. Guhl, S. Nolte, R. Ackermann, *In situ* investigation of carbon gasification using ultrabroadband coherent anti-Stokes Raman scattering, Appl. Phys. Lett. 119 (2021) 243905.
[11] Y. Ran, M. Junghanns, A. Boden, S. Nolte, A. Tünnermann, R. Ackermann, Temperature and gas concentration measurements with vibrational ultra-broadband two-beam femtosecond/picosecond coherent anti-Stokes Raman scattering and spontaneous Raman scattering, J. Raman Spectrosc. 50 (2019) 1268–1275.
[12] S.P. Kearney, Hybrid fs/ps rotational CARS temperature and oxygen measurements in the product gases of canonical flat flames, Combust. Flame 162 (2015) 1748–1758.
[13] S.A. Tedder, J.L. Wheeler, A.D. Cutler, P.M. Danehy, Width-increased dual-pump enhanced coherent anti-Stokes Raman spectroscopy, Appl. Opt. 49 (8) (2010) 1305–1313.
[14] M.P. Arroyo, R.K. Hanson, Absorption measurements of water-vapor concentration, temperature, and line-shape parameters using a tunable InGaAsP diode laser, Appl. Opt. 32 (30) (1993) 6104–6116.
[15] W.F. Murphy, The Rayleigh depolarization ratio and rotational Raman spectrum of water vapor and the polarizability components for the water molecule, J. Chem. Phys. 67 (12) (1977) 5877–5882.
[16] S. O'Byrne, P.M. Danehy, A.D. Cutler, S.A. Tedder, Dual-pump coherent anti-Stokes Raman scattering measurements in a supersonic combustor, AIAA J. 45 (2007) 922–933.
[17] R.J. Hall, J.A. Shirley, A.C. Eckbreth, Coherent anti-Stokes Raman spectroscopy: spectra of water vapor in flames, Opt. Lett. 4 (3) (1979) 87–89.
[18] R.J. Hall, J.A. Shirley, Coherent anti-Stokes Raman

spectroscopy of water vapor for combustion diagnostics, Appl. Opt. 37 (2) (1983) 196–202.
[19] F.M. Porter, D.R. Williams, Quantitative CARS spectroscopy of the v_1 of water vapour, Appl. Phys. B 54 (1992) 103–108.
[20] D.A. Greenhalght, R.J. Hall, F.M. Porter, W.A. England, Application of the rotational diffusion model to the CARS spectra of high-temperature, high-pressure water vapour, J. Raman Spectrosc. 15 (2) (1984) 71–79.
[21] E. Nordström, A. Bohlin, P.E. Bengtsson, Pure rotational Coherent anti-Stokes Raman spectroscopy of water vapor and its relevance for combustion diagnostics, J. Raman Spectrosc. 44 (10) (2013) 1322–1325.
[22] D.A. Long, The Raman effect: A Unified Treatment of the Theory of Raman Scattering by Molecules, 1st ed., John Wiley & Sons Ltd., 2002.
[23] M. Schmitt, G. Knopp, A. Materny, W. Kiefer, The application of femtosecond time-resolved coherent anti-stokes raman scattering for the investigation of ground and excited state molecular dynamics of molecules in the gas phase, J. Phys. Chem. A 102 (1998) 4059–4065.
[24] H. Skenderović, T. Buckup, W. Wohlleben, M. Motzkus, Determination of collisional line broadening coefficients with femtosecond time-resolved CARS, J. Raman Spectrosc. 33 (2002) 866–871.
[25] B.D. Prince, A. Chakraborty, B.M. Prince, H.U. Stauffer, Development of simultaneous frequency- and time-resolved coherent anti-Stokes Raman scattering for ultrafast detection of molecular Raman spectra, J. Chem. Phys. 125 (2006) 044502.
[26] B.D. Patterson, Y. Gao, T. Seeger, C.J. Kliewer, Split-probe hybrid femtosecond/picosecond rotational CARS for time-domain measurement of S-branch Raman linewidths within a single laser shot, Opt. Lett. 38 (22) (2013) 4566–4569.
[27] W. Meier, S. Prucker, M.-H. Cao, W. Stricker, Characterization of turbulent H_2/N_2/air jet diffusion flames by single-pulse spontaneous raman scattering, Combust. Sci. Technol. 118 (1996) 293–312.
[28] A. Bohlin, B.D. Patterson, C.J. Kliewer, Communication: simplified two-beam rotational CARS signal generation demonstrated in 1D, J. Chem. Phys. 138 (2013) 081102.
[29] N. Owschimikow, F. Königsmann, J. Maurer, P. Giese, A. Ott, B. Schmidt, N. Schwentnert, Cross sections for rotational decoherence of perturbed nitrogen measured via decay of laser-induced alignment, J. Chem. Phys. 133 (4) (2010) 044311.
[30] A.K. Patnaik, S. Roy, J.R. Gord, Saturation of vibrational coherent anti-Stokes Raman scattering mediated by saturation of the rotational Raman transition, Phys. Rev. A 87 (2013) 043801.
[31] C.J. Kliewer, A. Bohlin, E. Nordström, B.D. Patterson, P.-E. Bengtsson, T.B. Settersten, Time-domain measurements of S-branch N2-N2 Raman linewidths using picosecond pure rotational coherent anti-Stokes Raman spectroscopy, Appl. Phys. B 108 (2012) 419–426.
[32] C. Meißner, J.I. Hölzer, T. Seeger, Determination of N_2–N_2 and N_2–O_2 S-branch Raman linewidths using time-resolved picosecond pure rotational coherent anti-Stokes Raman scattering, Appl. Opt. 58 (10) (2019) 47–54.
[33] A. Bohlin, E. Nordström, B.D. Patterson, P.E. Bengtsson, C.J. Kliewer, Direct measurement of S-branch N_2-H_2 Raman linewidths using time-resolved pure rotational coherent anti-Stokes Raman spectroscopy, J. Chem. Phys. 137 (2012) 074302.
[34] J. Bonamy, D. Robert, J.M. Hartmann, M.L. Gonze, R. Saint-Loup, H. Berger, Line broadening, line shifting, and line coupling effects on N_2-H_2O stimulated Raman spectra, J. Chem. Phys. 91 (1989) 5916.
[35] L. Castellanos, F. Mazza, D. Kliukin, A. Bohlin, Pure-rotational 1D-CARS spatiotemporal thermometry with a single regenerative amplifier system, Opt. Lett. 45 (17) (2020) 4662–4665.
[36] F. Mazza, N. Griffioen, L. Castellanos, D. Kliukin, A. Bohlin, High-temperature rotational-vibrational O_2-CO_2 coherent Raman spectroscopy with ultra-broadband femtosecond laser excitation generated in-situ, Combust. Flame 44 (10) (2022) 1322–1325.
[37] S.P. Kearney, P.M. Danehy, Pressure measurements using hybrid femtosecond/picosecond rotational coherent anti-Stokes Raman scattering, Opt. Lett. 40 (17) (2015) 4082–4085.
[38] C.E. Dedic, A.D. Cutler, P.M. Danehy, Characterization of supersonic flows using hybrid fs/ps CARS, AIAA SciTech Forum (2019) 1–13.
[39] S.P. Kearney, D.R. Richardson, J.E. Retter, C.E. Dedic, P.M. Danehy, Simultaneous temperature/pressure monitoring in compressible flows using hybrid fs/ps pure-rotational CARS, AIAA SciTech Forum (2020) 1–8.
[40] D. Escofet-Martin, A.O. Ojo, J. Collins, N.T. Mecker, M.A. Linne, B. Peterson, Dual-probe 1-d hybrid fs/ps rotational CARS for simultaneous single-shot temperature, pressure and O_2/N_2 measurements, Opt. Lett. 45 (17) (2020) 4758–4761.
[41] F. Mazza, L. Castellanos, D. Kliukin, A. Bohlin, Coherent Raman imaging thermometry with *in-situ* referencing of the impulsive excitation efficiency, Proc. Combust. Inst. 38 (2021) 1895–1904.
[42] V.V Toro, A.V. Mokhov, H.B. Levinsky, M.D. Smooke, Combined experimental and computational study of laminar, axisymmetric hydrogen–air diffusion flames, Proc. Combust. Inst. 30 (2005) 485–492.
[43] J. A. Van Oijen, L. P. De Goey, Modelling of premixed laminar flames using flamelet-generated manifolds, Combust. Sci. Technol. 161 (1) (2000) 113–137.